

Finite element simulation of cross-laminated timber panels under compression perpendicular to plane

Rodrigo A. Benitez Mendes¹, Matheus Erpen Benincá¹, Inácio Benvegnu Morsch¹

¹Programa de Pós-Graduação em Engenharia Civil, Universidade Federal do Rio Grande do Sul
Av. Osvaldo Aranha, 99, 90035-190, Porto Alegre/RS, Brasil
rodrigo.btz@outlook.com, matheuseb@hotmail.com, morsch@ufrgs.br

Abstract. Cross-Laminated Timber (CLT) is a composite panel made up of structurally glued layers of wood lamellae stacked crosswise at 90° that has been standing out in the sustainable construction scenario. Among its main features, it is possible to highlight the excellent weight/strength ratio, when compared to other traditional construction materials, and great stiffness in both directions, provided by its orthogonal layerwise configuration. Frequently employed as a slab element in mid-rise and high-rise timber buildings, these engineered wood panels are often subjected to elevated compression loads perpendicular to plane in different loading conditions. This paper focus on the column-slab-wall load case of CLT slabs by proposing a numerical finite element model capable of simulating its elastoplastic nonlinear behavior under compression perpendicular to plane. An orthotropic constitutive model employing Hill's yield criterion combined with isotropic bilinear hardening was used, applied to 20-node solid hexahedral finite elements in Ansys Mechanical APDL software. The numerical results presented a good correlation with experimental data of non-edge-glued CLT panels, especially when gaps between lamellae were considered in the model's geometry. Finally, the anisotropic failure criterion of Tsai-Wu was assessed, showing potential in estimating the CLT layers' structural integrity under different load levels along the elastoplastic regime, even though it requires detailed mechanical characterization of wood as input data.

Keywords: cross-laminated timber, compression perpendicular to plane, finite element model.

1 Introduction

Since its conception in the early 1990s, Cross-Laminated Timber (CLT) panels are being known in the construction industry as one of the most preferred sustainable structural materials in multi-storey buildings (Karacabeily and Gagnon [1]). Iconic examples are the Brock Commons student residence in Vancouver and the mixed-use edifice Mjøstårnet in Norway, being both of them 18-storey tall and employing a hybrid structure combining glulam, CLT and concrete. CLT is a mass timber engineer product, made of lumber boards (lamellae) stacked crosswise at 90°, glued with structural adhesive, and pressed to form a solid, straight, rectangular panel. Its dimensions can reach up to 4 m wide and 18 m long, with thicknesses up to 50 cm, typically in 3, 5, or 7 layers, as presented in Fig. 1.

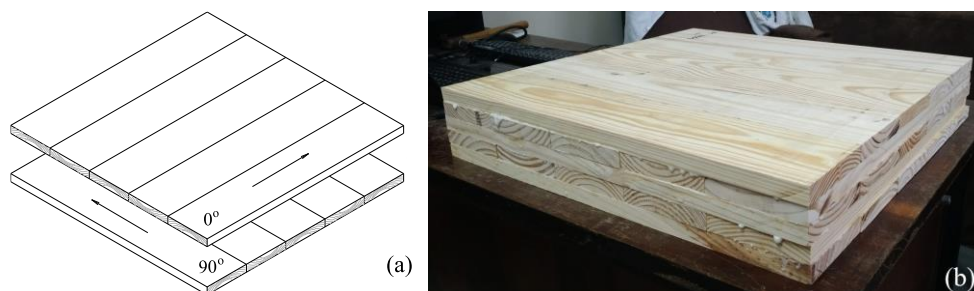


Figure 1. Cross-laminated Timber: (a) configuration of layers; (b) a 5-ply laboratory manufactured panel.

Another significant manufacturing aspect of these panels is that the structural adhesive is usually applied just on the lumber's faces and not on their edges, i.e., without edge-bonding/edge-gluing. This is done for practical and cost reasons, as well as for reducing potential dimensional stability problems, like wood checking, as stated by Karacabeily and Gagnon [1].

Being a relatively new structural element, it still lacks in the field of standardization and compatibility of existing regulations and standards. Nevertheless, in the meantime engineers have been relying on handbooks and manufacturer-issued specifications, based on the results of a great number of research projects carried so far. An ongoing point of study is CLT's mechanical behavior on compression perpendicular to plane and the strategies to model it with numerical simulations. This kind of loading is commonly present on CLT slabs of platform-type multi-storey buildings, where floors are completely or partially compressed between columns, walls, etc., opening a wide variety of possibilities and parameters that come into play regarding its structural response.

In this sense, Serrano and Enquist [2] simulated experimental tests of line-compressed CLT, employing a linear elastic Finite Element (FE) model. They highlighted the importance of discretizing the lamellae on layers and the need for an orthotropic plastic material model. Salzmann [3] conducted punctual compression tests on CLT panels, and among other inferences based on a linear elastic FE model, he concluded that compressive stiffness is strongly influenced by the location of lumber in relation to the tree's pith. Bogensperger et al. [4] studied differences between glulam and CLT with a FE model applying an elastoplastic relationship only on the local material axis perpendicular to plane. They determined that the interlocking effect caused by the cross layering has a considerable benefic effect on the compressive stiffness and strength parameters.

In the context of mentioned researches, Mendes [5] carried out compression perpendicular to plane experimental tests on non-edge-bonded CLT panels, considering a column-slab-wall load configuration. This paper proposes to investigate these tests on a numerical basis, by proposing FE models capable of describing the elastoplastic behavior of such CLT panels subjected to this kind of loading, mainly focusing on the effect of intralaminar gaps. Tests results were taken for validation purposes. Additionally, an anisotropic failure criterion was evaluated in this context and contrasted with experimental results with regard to the structural safety of panels.

2 Numerical model

Two finite element (FE) models were developed in ANSYS Mechanical APDL software, v. 19.3, to simulate experimental tests carried out in a previous study by Mendes [5]: Model I considered perfect edge-bonding of lamellae; Model II considered intralaminar gaps of 1 mm i.e., no edge-bonding, as shown in Fig. 2. Both of them employed hexahedral 20-node SOLID186 elements, with the same constitutive model and input parameters. Blue layers are longitudinal in the x -axis, while cyan layers are longitudinal in the y -axis.

Wood is a heterogeneous and strongly anisotropic material, i.e., its properties depend on the tree trunk's anatomical direction. This anisotropy can be idealized as an orthotropy, defined by three axes: L , along the wood grains; R and T , being radial and tangential, respectively, to the annual rings and perpendicular to grain. Hence, this is the usual local coordinate system associated with wood, and also the herein adopted. Moreover, it's common practice to indistinctly consider R and T directions, as their magnitude difference is negligible in comparison with L and standards also don't distinguish them [1,6]. This condition intensifies on engineered wood elements, as the homogeneity increases with the combination of wood pieces from the same batch/strength class.

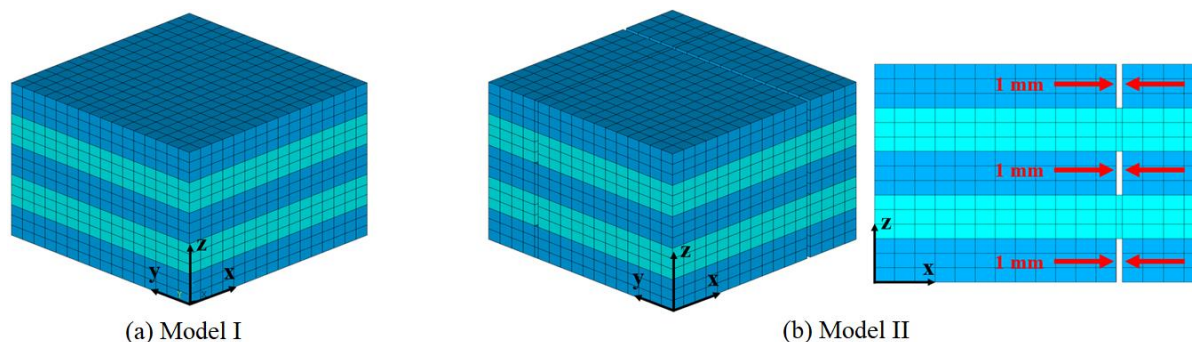


Figure 2. FE models of a series A cube: (a) Model I; (b) Model II and a close-up view of the intralaminar gaps.

2.1 Material parameters

The constitutive model adopted an elastoplastic nonlinear transversely isotropic material model for wood, using Hill's yield criterion [7] combined with bilinear isotropic hardening. Elastic and plastic parameters were adopted according to the solid wood characterization conducted by Mendes [5], and are presented in Tab. 1 and 2. The CLT panels of Mendes [5] were manufactured with two different batches of *Pinus elliottii*, being the lumber of Batch 1 more juvenile than the one of Batch 2. Poisson's ratios were taken from Kretschmann [8] for Slash pine. Shear moduli were estimated with classical standardized equations for softwood species, according to Karacabeily and Gagnon [1]. Properties used to describe the yield criterion, flow, and hardening rule were adopted taking previous researches as guidance, including Jasieńko and Kardysz [9], Nowak et al. [10], where σ_o is the reference yield stress, T the tangent modulus, and R_{ij} Hill's yield stress ratios. A detailed explanation of the implementation of this constitutive model is given in the software's manual of ANSYS [11].

Table 1. Elastic material parameters adopted for the numerical models.

Batch	E_L (MPa)	E_T (MPa)	E_R (MPa)	G_{LT} (MPa)	G_{TR} (MPa)	G_{LR} (MPa)	ν_{LT}	ν_{TR}	ν_{LR}
1	3,700	340	340	230	23	230	0.418	0.387	0.418
2	10,300	280	280	640	64	640	0.418	0.387	0.418

Table 2. Plastic material parameters adopted for the numerical models.

Series	Specimen	σ_o (MPa)	T (MPa)	R_{xx}	$R_{xy} = R_{yz}$	R_{xz}
A	Cube	3.9	11	5	0.9	0.2
	Plate	4.2	21	5	0.8	0.4
B	Cube	3.5	6	10	1.4	0.7
	Plate	3.5	9	10	1.4	0.7
C	Cube	3.2	6	10	1.5	0.6
	Plate	3.5	14	10	1.4	0.7

2.2 Geometry of specimens and boundary conditions

The CLT panels tested by Mendes [5] had three different layer configurations: series A with 21 mm thick 5 layers of Batch 1 wood, and series B and C with 35 mm thick layers of Batch 2 wood, stacked in 3 and 5 layers, respectively. The simulations regarded uniformly loaded and supported cubes on one hand, and plates on a column-slab-wall load configuration on the other, as shown in Fig. 3.

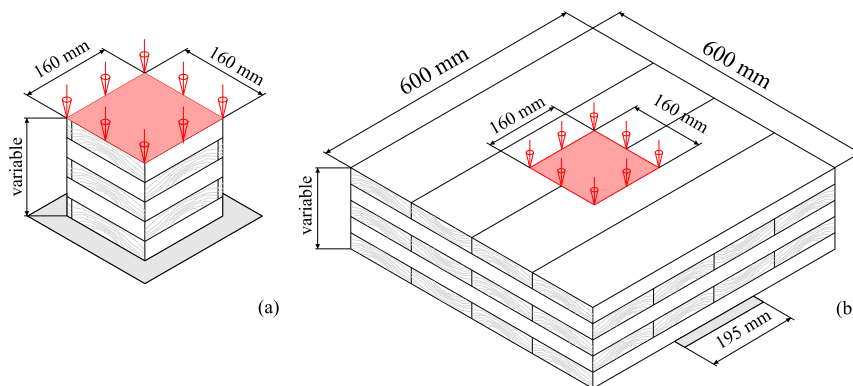


Figure 3. Experimental configuration of simulated tests: (a) cubic specimen; (b) plate specimen.

In the tests, a thick steel plate was used to apply compression on the specimens. Here the load was applied directly on the CLT by imposing vertical displacements on the loaded area. Double symmetry was employed to

reduce computational cost. The boundary condition implemented are illustrated in Fig. 4. Equivalent conditions were applied to simulate the uniformly loaded cube. Validation was made in terms of load-displacement curves and strength values following the EN 408 standard [6], considering the loaded area for its calculus. Vertical displacements were measured on the upper central node of the models.

After a mesh refinement study, FE meshes adopted the following characteristics: 3 elements per layer thickness; maximum element size of 10 mm and 15 mm for the cube and plate models, respectively; 4,080 elements – 19,620 nodes and 5,720 elements – 28,059 nodes for the series A cube and plate models, respectively, and similarly for series B and C.

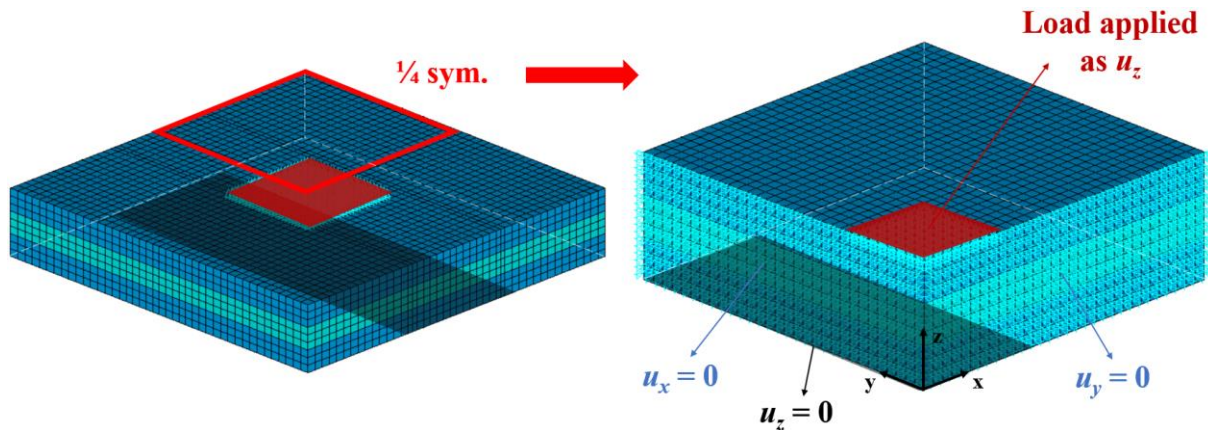


Figure 4. Boundary conditions of FE models: series B plate example with $\frac{1}{4}$ symmetry.

3 Results and discussion

3.1 FE Models' validation

An experimental and numerical comparison example of load-displacement curves is shown in Fig. 5 for series B specimens. It can be noted that Model I and II behaved the same manner with respect to the cube specimens, both having a good correlation with experimental data. This can be expected since there is no redistribution of stress along thickness when the load is uniformly applied, hence gaps have no influence. On the contrary, regarding plate specimens, Model I clearly diverges from the test curves, showing a much stiffer behavior; whereas Model II was able to capture the yielding moment and hardening evolution with good precision. This is probably due to the severe reduction in stress dispersion along the thickness of CLT, causing stress concentration zones around the intralaminar gaps, and therefore forcing the material to reach yielding much faster. This elevated stress gradient can be seen in Fig. 6 for the series A plate for applied force of 154,750 kN.

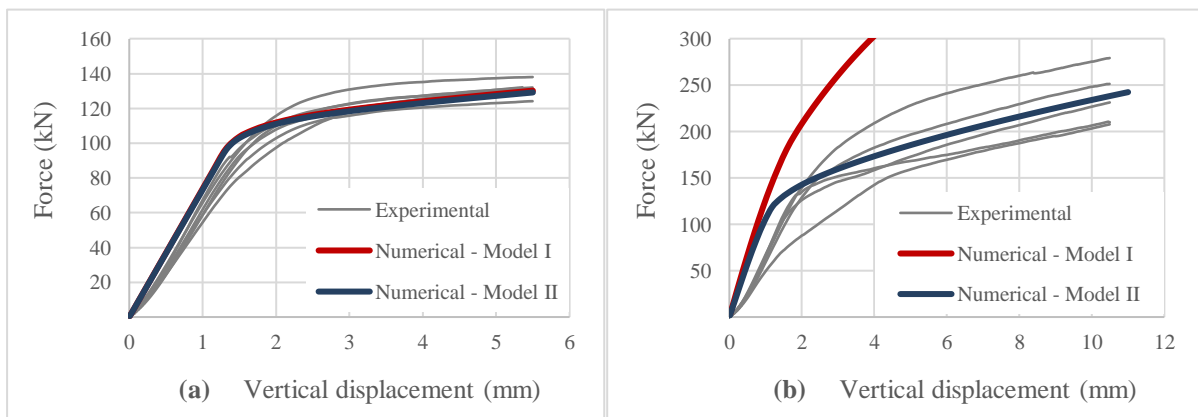


Figure 5. Experimental and numerical load-displacement curves of series B specimens: (a) cubes; (b) plates

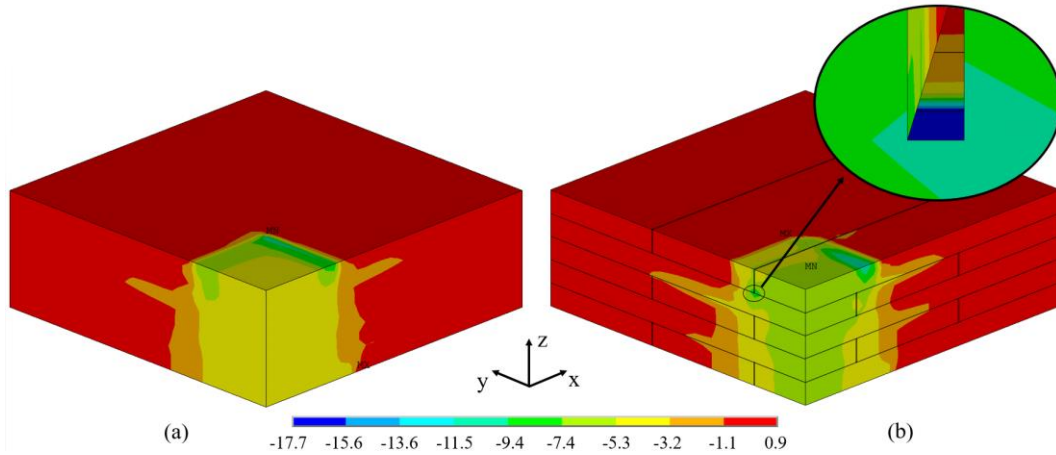


Figure 6. Contour plot of σ_3 principal stresses (MPa) of series A plate: (a) Model I; (b) Model II.

A complete comparison of CLT's compressive strength perpendicular to plane ($f_{c,90,CLT}$) for cubes and plates of all series is presented on Tab. 3. Again, the difference between models is negligible concerning the cubes, and with an error of less than 5 % in relation to experimental determinations. However, regarding the plates, their overall difference was 40 %, owing to the fact that this parameter depends fundamentally on the moment yielding begins. Consequently, the average error of Model I was 45 % above the experimental median, and of Model II was -12 %, providing rather conservative estimations, but still between maximum and minimum observations.

Table 3. Comparison of experimental and numerical strength in compression perpendicular to plane of CLT.

Series	Specimen	$f_{c,90,CLT}$ (MPa)					Error (%)		
		Model I	Model II	Exp. Min.	Exp. Median	Exp. Max.	Model I	Model II	Model I vs. II
A	Cube	4.56	4.49	4.08	4.39	4.94	3.94	2.20	1.67
	Plate	8.45	6.05	6.02	6.40	7.91	32.08	-5.50	28.45
B	Cube	4.54	4.51	4.51	4.68	5.10	-2.95	-3.66	0.73
	Plate	10.59	5.79	5.72	5.96	7.94	77.75	-2.88	45.36
C	Cube	4.11	4.10	3.95	4.10	4.49	0.16	0.03	0.14
	Plate	12.02	6.74	6.32	9.28	10.63	29.55	-27.39	43.95

Errors of Models I and II are calculated in relation to the experimental median.

3.2 Failure assessment with Tsai-Wu's criterion

The Tsai-Wu failure criterion, detailed in Tsai and Hahn [12], was applied to evaluate the integrity of the series C plate along load-steps in terms of the failure index (I_F), i.e., regions with a value above 1 indicate structural failure. The implementation of this criterion is detailed in ANSYS' manual [11]. As the solid wood's characterization of Mendes [5] only comprised compressive tests, remaining shear and tension strength parameters were extracted from NBR 7190 standard [13] for *Pinus elliottii*, as shown in Tab. 4. Transverse isotropy was also considered for these parameters.

Table 4. Wood strength parameters (MPa) employed in the Tsai-Wu criterion.

$f_{t,0}$	$f_{c,0}$	$f_{t,90}$	$f_{c,90}$	$f_{v,0}$	$f_{v,90}$
+ 52.0	- 40.4	+ 2.5	- 3.9	6.0	3.0

The model predicted a localized failure mode that resembles with test's observations of Mendes [5], as shown in Fig. 7a. The first region to reach $I_F = 1$ was around the vertex of the loaded area for an applied force of 87 kN, still in the elastic domain (see Fig. 7b). Since the load-displacement curve is plotted for the upper central node, it

reaches yielding about 40 % later (~124 kN) because it isn't a stress concentration point as a sudden change in geometry naturally is (e.g., vertex of loaded area). At $f_{c,90,CLT}$ level, the upper central region reaches values between $0.65 \leq I_F \leq 0.97$, agreeing quite well with EN 408 strength criterion [6]. Tsai-Wu's failure criterion appears to be promising regarding CLT, although it should be noted that it requires a demanding wood characterization test programme (9 strength parameters considering orthotropy) to be reliably exploited.

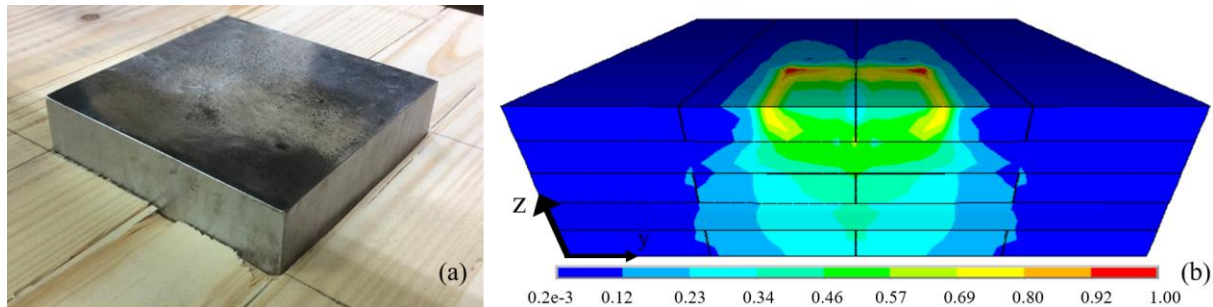


Figure 7. Plate's compressive failure: (a) Test by Mendes [5]; (b) Tsai-Wu's I_F contour plot on YZ cross section.

3.3 Interpenetration and model refinement

Despite reaching a good correlation with experimental results, FE mesh interpenetration was observed on interlaminar gaps of Model's II plate simulations. Two phenomena trigger this event: (i) as friction between CLT and the steel plate wasn't considered on the loaded area, gaps' edges are free to move horizontally during compression; and also (ii) due to the Poisson's effect. Therefore, it is expected that the small 1 mm gaps should close, and afterwards, lateral faces of the lamellae could interpenetrate each other, since contact elements were not used. Fig. 8 shows the moment at which interpenetration begins.

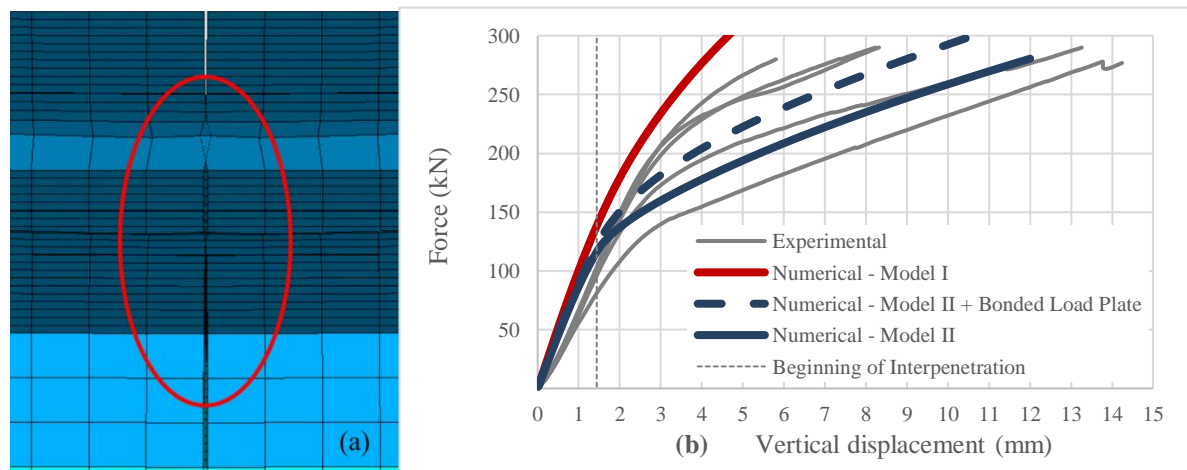


Figure 8. FE mesh interpenetration: (a) close-up view of the loaded area; (b) Effect of bonded load plate boundary condition on series C plate.

Also, Fig. 8 shows the effect of nulling the horizontal displacements of the loaded area nodes: this boundary condition accounts as if the steel plate was perfectly bonded on the CLT specimen, delivering a stiffness to the gaps beneath the loaded area that hinders the phenomenon (i), mentioned above. With this new condition, interpenetration delays by 40 % in relation to the results with the original boundary conditions. It is expected that considering contact friction at the load interface between the steel plate and CLT, by applying interface elements with a coefficient of friction, would bring an intermediate curve to the ones corresponding to the completely free and perfectly bonded load plate condition. Furthermore, intralaminar wood-wood contact elements could also be added to this model in order to avoid interpenetration to happen. Future investigations have to appraise the potential benefits of these refinements against the natural increase of computational cost they would require.

4 Conclusions

Two FE numerical models were developed to simulate the elastoplastic behavior of CLT in compression perpendicular to plane, one considering edge bonded layers and the other accounting for small intralaminar gaps. These models were applied to simulate experimental tests of a previous work. From the results, the following main conclusions can be drawn:

- Model II, accounting for intralaminar gaps, agreed better than Model I with the experimental results of non-edge-bonded CLT specimens. However, FE mesh interpenetration was observed;
- Intralaminar gaps have a strong influence on the numerical results, represented by a significant earlier yielding point on the load-displacement curve and a small decrease in stiffness;
- The constitutive model of Hill's yield criterion combined with isotropic bilinear hardening was able to accurately predict the characteristic bilinear curve of experimental tests, showing potential for its application in simulating CLT's mechanical behavior under compression perpendicular to plane;
- Tsai-Wu's failure criterion presents as an interesting tool to assess the structural integrity of each CLT layer under increasing load levels along the elastoplastic regime. However, it requires extensive characterization of wood strength parameters in order to deliver more reliable prognoses.
- The FE mesh interpenetration observed needs further study. Effects of friction on the load interface, as well as contact elements between wood on interlaminar gaps could be added to the model in future studies.

Acknowledgments. The authors are grateful to CAPES for the financial support of this research, as well as to CEMACOM/UFRGS for providing the infrastructure for the development of this work.

Authorship statement. The authors hereby confirm that they are the sole liable persons responsible for the authorship of this work, and that all material that has been herein included as part of the present paper is either the property (and authorship) of the authors, or has the permission of the owners to be included here.

References

- [1] E. Karacabeily and S. Gagnon. *Canadian CLT Handbook: 2019 Edition*. FPInnovations, 2019.
- [2] E. Serrano and B. Enquist, "Compression strength perpendicular to grain of Cross-Laminated Timber (CLT)". In: A. Ceccotti (ed.), *Proceedings of the XI WCTE – World Conference on Timber Engineering*, pp. 7.
- [3] C. Salzmann. Ermittlung von Querdruckkenngrößen für Brettsper Holz (BSP). Master's thesis, Graz University of Technology, 2010. [in German]
- [4] T. Bogensperger, M. Augustin and G. Schickhofer, "Properties of CLT-Panels exposed to compression perpendicular to their plane". In: R. Görlacher (ed.), *International Council for Research and Innovation in Building and Construction, Working Commission W18 – Timber Structures, Meeting 44 (CIB-W18/44-12-1)*, pp. 215-231.
- [5] R. A. B. Mendes. *Structural behaviour of Cross-Laminated Timber panels subjected to out-of-plane loading: an experimental and numerical approach*. Master's thesis, Federal University of Rio Grande do Sul, 2020. [in Portuguese]
- [6] AENOR. *UNE-EN 408: Estructuras de madera – Madera aserrada y madera laminada encolada para uso structural. Determinación de algunas propiedades físicas y mecánicas*. Madrid, 2011. [in Spanish]
- [7] R. Hill, "A theory of the yielding and plastic flow of anisotropic metals". *Proceedings of the Royal Society London A*, vol. 193, n. 1033, pp. 281-297, 1948.
- [8] D. E. Kretschmann. *Mechanical properties of wood*. In: *Wood Handbook – Wood as an engineering material*. Forest Products Laboratory. Centennial ed., 2010.
- [9] J. Jasiński and M. Kardysz, "Deformation and Strength Criteria in Assessing Mechanical Behavior of Joints in Historic Timber Structures". In: ICOMOS International Wood Committee (ed.), *Proceedings of the 16th IWC international conference and symposium*, pp. 63-79.
- [10] T. P. Nowak, J. Jasiński and Dariusz Czepizak, "Experimental tests and numerical analysis of historic bent timber elements reinforced with CFRP strips". *Construction and Building Materials*, vol. 40, pp. 197-206, 2014.
- [11] ANSYS, Inc. ANSYS help system: version 19.3. Canonsburg, 2018.
- [12] S. W. Tsai and T. H. Hahn. *Introduction to Composite Materials*. Technomic Publishing Company, 1980.
- [13] ABNT. *NBR 7190: Projeto de Estruturas de Madeira*. Rio de Janeiro, 1997. [in Portuguese]